

Axis-inducing activities and cell fates of the zebrafish organizer

Leonor Saude¹, Katie Woolley², Paul Martin², Wolfgang Driever³ and Derek L. Stemple^{1,*}

¹Division of Developmental Biology, National Institute for Medical Research, Mill Hill, London NW7 1AA, UK

²Department of Anatomy and Developmental Biology, University College London, Gower Street, London, WC1E 6BT, UK

³Department of Developmental Biology, Biologie 1, University of Freiburg, Hauptstraße 1, D-79104 Freiburg, Germany

*Author for correspondence (e-mail: dstempl@nimr.mrc.ac.uk)

Accepted 4 June; published on WWW 20 July 2000

SUMMARY

We have investigated axis-inducing activities and cellular fates of the zebrafish organizer using a new method of transplantation that allows the transfer of both deep and superficial organizer tissues. Previous studies have demonstrated that the zebrafish embryonic shield possesses classically defined dorsal organizer activity. When we remove the morphologically defined embryonic shield, embryos recover and are completely normal by 24 hours post-fertilization. We find that removal of the morphological shield does not remove all *gooseoid*- and *floating head*-expressing cells, suggesting that the morphological shield does not comprise the entire organizer region. Complete removal of the embryonic shield and adjacent marginal tissue, however, leads to a loss of both prechordal plate and notochord. In addition, these embryos are cyclopean, show a significant loss of floor plate and primary motorneurons and display disrupted somite patterning. Motivated by apparent discrepancies in the

literature we sought to test the axis-inducing activity of the embryonic shield. A previous study suggested that the shield is capable of only partial axis induction, specifically being unable to induce the most anterior neural tissues. Contrary to this study, we find shields can induce complete secondary axes when transplanted into host ventral germ-ring. In induced secondary axes donor tissue contributes to notochord, prechordal plate and floor plate. When explanted shields are divided into deep and superficial fragments and separately transplanted we find that deep tissue is able to induce the formation of ectopic axes with heads but lacking posterior tissues. We conclude that the deep tissue included in our transplants is important for proper head formation.

Key words: *Danio rerio*, Zebrafish, Organizer, Embryonic shield, Regeneration, *gooseoid*, *floating head*, Secondary axis, Notochord, Prechordal plate, Floor plate, Neural induction

INTRODUCTION

The vertebrate body plan is established by a series of inductive interactions and cellular rearrangements. Cellular and molecular mechanisms underlying these processes are perhaps best understood for amphibia where axis formation is thought to occur in a series of discrete steps (for a recent review, see Harland and Gerhart, 1997). Localization of maternal determinants to dorsal vegetal cells in the embryo creates a primary organizing center, the Nieuwkoop center (Vincent et al., 1986; Rowning et al., 1997). After the mid-blastula transition, zygotic gene products from the Nieuwkoop center induce the Spemann organizer to form in the overlying equatorial region.

The Spemann organizer is a region of the amphibian gastrula that will induce a second body axis upon transplantation to ventral or lateral regions of a host embryo. The Spemann organizer provides signals that dorsalize mesoderm, induce convergent-extension movements in ectoderm and mesoderm and specify neurectoderm (Spemann and Mangold, 1924; Smith and Slack, 1983; Keller et al., 1992; Doniach et al., 1992). In an induced secondary axis, the donor organizer contributes predominantly to axial tissue, particularly

notochord and prechordal plate (Spemann and Mangold, 1924; Harland and Gerhart, 1997). Functional equivalents of the amphibian Spemann organizer have been identified in other vertebrates by transplantation experiments (Waddington, 1932; Beddington, 1994). In the zebrafish and other teleost fish, the embryonic shield possesses organizer activity (Oppenheimer, 1936; Shih and Fraser, 1996). At the time the embryonic shield becomes morphologically apparent it consists of superficial epiblast and deep hypoblast layers that rest on the yolk cell and are covered by a tight epithelium called the enveloping layer (EVL). The structure of the shield is also manifest in differential gene expression. For example, epiblast cells of the shield express the *floating head* (*flh*) gene (Talbot et al., 1995), whereas the deeper hypoblast cells express *gooseoid* (*gsc*) (Stachel et al., 1993). A recent study has shown that *gsc*-expressing cells are fated to give rise to prechordal plate, whereas *flh*-expressing cells give rise to notochord (Gritsman et al., 2000).

Characterization of the teleost organizer by various researchers has led to similar but distinct conclusions. In her pioneering work, Oppenheimer showed that transplanted pieces of embryonic shield from *Perca* were able to induce a complete secondary axis in host embryos (Oppenheimer, 1936,

1953). More recently Shih and Fraser (1996) reported that pieces of shield grafted to host embryos were able to induce secondary axes but were never able to induce anteriormost structures, such as eyes. Similarly, in mouse node grafting experiments secondary axes were found to lack anterior structures (Beddington, 1994). Subsequently the anterior region of the visceral endoderm (AVE) was implicated as an organizer of anterior neurectoderm (Thomas and Beddington, 1996; Varlet et al., 1997; Tam and Steiner, 1999). These data suggested the possibility that anterior specification in zebrafish, similar to mouse, requires spatially distinct activities. The fact that the embryonic shield of another teleost fish, *Perca*, is capable of inducing complete secondary axis formation, however, suggests that part of the organizer's activities were possibly lost in previous zebrafish shield transplantation experiments (Shih and Fraser, 1996).

Recent genetic work provides some insight into the relationship between the embryonic shield and organizer activity. In particular, mutations in the zebrafish *bozozok* (*boz*) locus affect both shield morphology and the development of shield-derived tissues. The most severely affected *boz* mutants have a reduced embryonic shield, which correlates with the reduction of *gsc* and *flh* gene expression (Fekany et al., 1999). Later in development, severely affected *boz* mutant embryos display a complete loss of the axial tissues: notochord and prechordal plate. The *boz* gene product is a homeodomain-containing transcription factor whose expression is limited to the yolk syncytial layer (YSL) and dorsal marginal cells. Functionally, these *boz*-expressing cells appear to act as the teleost equivalent of the Nieuwkoop center (Fekany et al., 1999). Thus there are two possible modes of *boz* action: either it is responsible for induction of organizer activity per se, or *boz* is primarily responsible for the specification of the tissues that normally derive from the shield region, specifically the axial mesendoderm and floor plate. Hence, whether the AP patterning defects are a consequence of the early loss of shield tissue or an independent event associated with the establishment of organizer activity is a question raised by the *boz* mutation. In order to draw a distinction between organizer activity and the cell fates of organizer-derived tissue in wild-type embryos, we developed a new method of tissue removal and transplantation that would allow us to completely remove the organizer of zebrafish gastrulae. We could then compare the phenotype of the mechanical removal of organizer to the effect of the *boz* mutation, while testing the ability of the removed tissue to induce secondary axes.

We find that removal of the morphological shield is not sufficient to prevent formation of normal shield derivative tissues, namely prechordal plate and notochord. Indeed we find that when removal is limited to the morphological shield, derivative tissues can regenerate, producing completely normal embryos by 24 hours post-fertilization (hpf). Complete removal of the shield region, however, prevents the formation of the normal shield derivative tissues. Complete shield-ablated embryos also fail to properly pattern the CNS, displaying a loss of floor plate and holoprosencephaly. These defects phenocopy the *boz* mutation. Since axes form with normal anterior-posterior identities in complete shield-ablated embryos, we conclude that *boz* acts primarily to specify axial mesendoderm and not to induce organizer activities per se.

When transplanted we find that extirpated shields are able

to induce a complete secondary axis and to contribute axial tissues, including floor plate. Our data differ from earlier reports, both in the extent of tissues missing after complete shield ablation and in the inductive capacity of shields in transplants. Finally, when deep and superficial regions of the shield were separately tested for organizer activity, we found deep shield tissue was able to induce secondary axes consisting entirely of head structures and superficial shield tissue was able to induce secondary axes lacking the most anterior structures.

MATERIALS AND METHODS

Embryo collection

Zebrafish (*Danio rerio*) embryos were raised at 28°C in 0.3× Danieau solution (1× Danieau: 58 mM NaCl, 0.7 mM KCl, 0.4 mM MgSO₄, 0.6 mM Ca(NO₃)₂, 5 mM Hepes, pH 7.6) (Shih and Fraser, 1996). Approximate stages are given in hours post-fertilization (hpf) at 28°C according to Kimmel et al. (1995).

Embryo labeling and microsurgery

Donor embryo chorions were removed by 4-minute incubation in 0.5 mg/ml Pronase (Sigma, P-8811) in 0.3× Danieau solution. Donors were labeled at the 1-4 cell stage by microinjection into the yolk with 5% fluorescein or rhodamine dextran (Molecular probes, D-1817) and 5% biotin dextran in 0.2 M KCl (Molecular Probes, D-1956). Embryos were injected in ramps made of 2% agarose in 0.3× Danieau solution. Injected embryos were cultured at 28°C in 2% agarose-coated dishes. Chorions of host embryos were removed with watchmaker's forceps shortly before transplantation.

Transplantation pipettes were pulled from 1 mm borosilicate glass capillaries (World Precision Instruments, 1B100-4) and cut with a diamond pencil to an inner diameter of approx. 200 µm (Fig. 1). A sharp inner edge is optimal and the plane of the cut was orthogonal to the long axis of the pipette. The pipettes were initially filled with medium and then loaded into a pipette holder filled with mineral oil. The pipette holder (World Precision Instruments, 5430-10), carried by a 3-axis micromanipulator (Narishige, MN-153), was connected, via a continuous column of mineral oil, to a 50 µl Hamilton syringe driven by micrometer-controlled syringe pump (Stoelting, 51218).

Transplantation experiments were performed at 19-21°C in 1× Danieau solution containing 5% penicillin/streptomycin (Gibco-BRL, 15140-114). Donor and host embryos were loaded into transplantation wells that had been preformed with an acrylic mould in 2% agarose 1× Danieau solution. Transplantation wells were 1.0 mm deep by 1.0 mm wide, with the bottom surface of the well sloping from the back wall of the well approximately 1.3 mm to the surface of the agarose.

To remove shield tissue, donor embryos were oriented such that the shield faced the pipette tip and the transplantation pipette was placed over the shield (Fig. 1A). Shield tissue was gently drawn in and out of the pipette generally 3 or 4 times until the yolk cell and shield tissue became separated (Fig. 1B). Two tissue removals were necessary for complete shield region ablation (see Results).

To transplant the shield tissue, hosts were oriented so that the site of transplantation was 180° from the host shield. With the donor shield in the pipette, the tip of the pipette was placed onto the host embryo, at the margin, and a piece of ventral tissue was removed and discarded (Fig. 1C). The donor shield was pushed to the tip of the pipette, which was placed over the hole in the host embryo (Fig. 1D). The donor shield was very gently expelled into the host embryo. Typically, the EVL of the host inflated a little, making space for the donor tissue. For acceptable transplants, the donor shield tissue became trapped under the EVL either directly beneath or immediately adjacent to the hole. Transplanted embryos were left in the transplantation well for about 10 minutes to recover then transferred to 0.3× Danieau containing 5% penicillin/streptomycin on 2% agarose, 0.3× Danieau

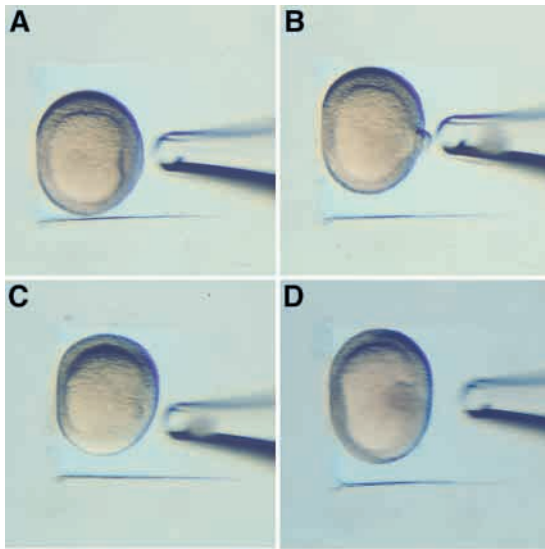


Fig. 1. Experimental technique for shield removal and transplantation. Shield removal is accomplished by aspiration from a 6 hpf embryo previously labeled with a lineage tracer dye. (A) The donor embryo is positioned with the shield facing the pipette. (B) The shield is removed from the embryo by gentle trituration. (C) Prior to transplantation, an equivalent size piece of host ventral tissue is removed. (D) The donor shield is then inserted under the EVL in the ventral side of a host embryo.

for overnight culture. The fate of transplanted embryonic tissues was recorded by direct fluorescence observation or by staining with avidin-HRP (Vector Labs). Embryos were fixed at 4°C overnight in 4% paraformaldehyde in phosphate-buffered saline (PBS). For staining, embryos were incubated for 1 hour at room temperature with avidin-HRP complex in PBS, 0.1% Tween 20 (PBT), then washed 5× with PBT and incubated in 0.4 mg/ml diaminobenzidine in PBT for 1 hour at room temperature. The staining reaction was initiated by the addition of a fresh solution of 0.4 mg/ml DAB/PBT containing 0.003% of H₂O₂. After stopping the reaction with several washes of PBT, embryos were refixed in 4% paraformaldehyde/PBS. Embryos were cleared with 20% glycerol/80% PBS, 50% glycerol/50% PBS and stored at 4°C in 80% glycerol/20% PBS.

In some experiments explanted shields were further manipulated before transplantation in order to separate deep and superficial shield tissue. Explanted shields were laid on a flat agarose surface, held with a hair loop, while several cuts were made with an eyebrow hair knife (Fig. 10B). Two vertical cuts were made to divide the shield into three equal pieces. The central piece was discarded. The shield fragment originally adjacent to the YSL (i.e. the deep fragment) was further trimmed by two lateral cuts to minimize contamination with superficial cells. Fragments were then transplanted as described for whole shields above.

Whole-mount in situ hybridization

Whole-mount in situ hybridizations were performed essentially as described by Thisse and Thisse (1998).

Electron microscopy

Embryos for scanning electron microscopy were fixed overnight in half-strength Karnovsky fixative (Karnovsky, 1965), rinsed in 0.1 M cacodylate buffer, and postfixed in ice-cold 1% osmium tetroxide in 0.1 M cacodylate buffer. Samples were then dehydrated through graded concentrations of ethanol, rinsed twice in acetone, and critical-point dried in CO₂, before being sputter-coated with gold and viewed with a Philips 515 scanning electron microscope.

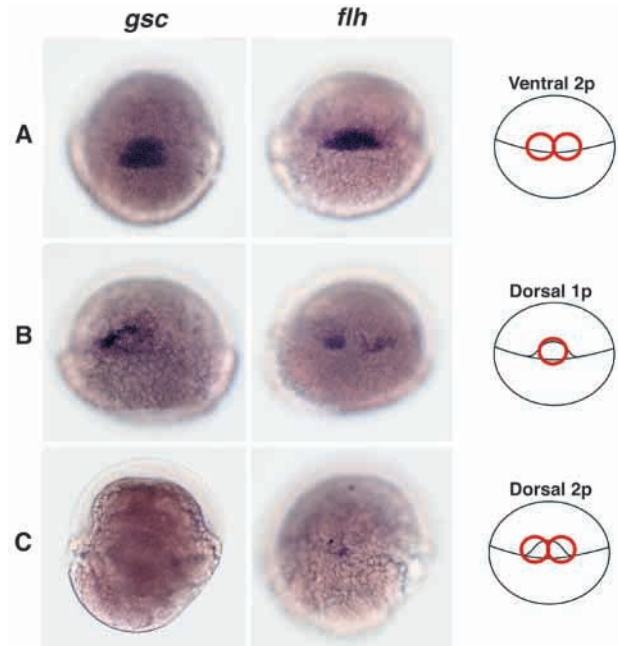


Fig. 2. Expression of *gsc* and *flh* in shield-ablated embryos. (A) As a control, two pieces of ventral germ-ring were removed. The control embryos show normal *gsc*- and *flh* expression. (B) The morphologically defined shield is removed using a glass pipette, roughly the diameter of an embryonic shield. This is insufficient to remove all the *gsc*- and *flh*-expressing cells, as confirmed by in situ hybridization. (C) When two pieces of dorsal margin are ablated the *gsc*- and *flh*-expressing cells are completely removed. All panels show dorsal views of 6 hpf embryos with anterior up.

Photomicrography

Live fluorescence images were obtained using a Leica compound microscope fitted with a Princeton Instruments, MicroMax cooled-CCD camera. MetaMorph image processing software was used to acquire images and overlay fluorescence and Nomarski images. Whole-mount in situ hybridization images were obtained using a Zeiss Axiophot microscope fitted with a Kodak DCS420 digital camera.

RESULTS

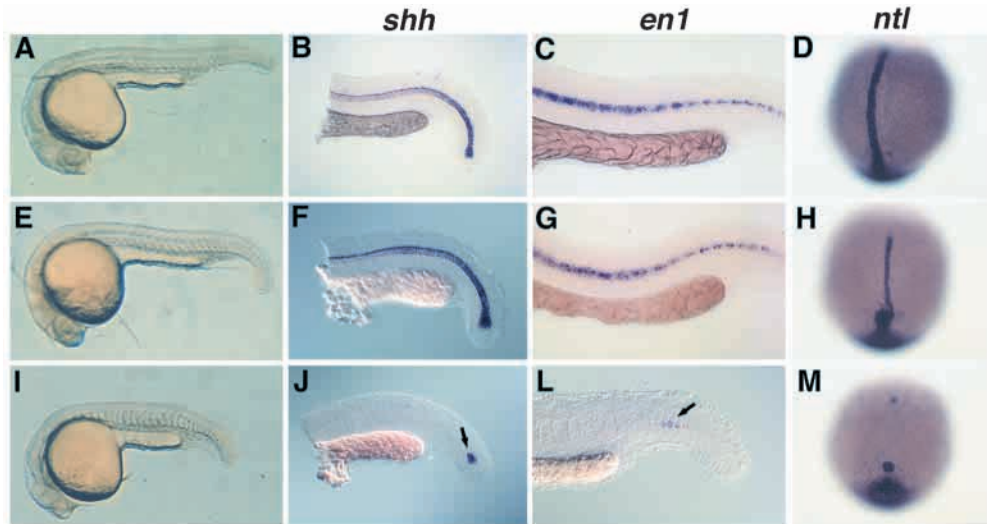
Developmental consequences of shield removal

Axial defects

Shield removal was achieved by aspiration with a pipette of inner diameter approximately the size of the shield (Fig. 1A, B). We found, however, that removal of the morphological shield did not eliminate all tissue expressing the organizer-specific genes *gsc* and *flh* (Fig. 2B). We therefore conclude that extirpation of the morphological shield only partially removes axial mesendoderm progenitors. Complete shield-region ablation, that is complete removal of tissue expressing *gsc* and *flh*, was achieved by extirpating two adjacent pieces from the dorsal margin (Fig. 2C). To assess the developmental consequences of partial (morphological shield only) and complete (morphological shield and adjacent marginal tissues) shield removal, experimental embryos were cultured until 24 hpf and analyzed.

Embryos that had undergone morphological shield

Fig. 3. Complete shield removal leads to axial defects. (A-D) Control embryos, where two pieces of ventral germ-ring were removed. (E-H) Removal of the morphological shield leads to normal development of axial structures, as revealed by in situ hybridization with the molecular markers *shh*, *en1* and *ntl*. (I) Complete shield removal leads to lack of notochord and chevron shaped somites. (J,M) The absence of differentiated notochord cells in complete shield-ablated embryos is confirmed by the reduction in *shh* and *ntl* expression. The arrow identifies residual *shh*-expressing cells in the tail bud. (L) Expression of *en1* is not detected in muscle pioneer cells of notochordless embryos, as revealed by in situ hybridization. The arrow identifies some *en1*-expressing cells adjacent to residual notochord cells. (A,C,E,G,I,L) Lateral views of 24 hpf embryos with anterior to the left. (B,F,J) Lateral views of 18 hpf embryo with anterior to the left. (D,H,M) Dorsal view of 2-somite-stage embryos with anterior up.



removal developed normally in 71% of the cases ($n=75$) (Fig. 3E-H). By contrast, only 5% of embryos subjected to complete shield removal developed normally ($n=70$). In all cases of ventral margin removal embryos developed normally ($n=52$) (Fig. 3A-D).

Complete shield removal produced embryos that were generally shorter than control embryos (Fig. 3I). By morphological criteria, these embryos completely lacked the axial tissues: notochord, floor plate and hatching gland (Fig. 3I). Axial expression of *sonic hedgehog* (*shh*) and *no tail* (*ntl*) RNA were significantly reduced in complete shield-ablated embryos, consistent with the morphological deficiencies in notochord and floor plate (Fig. 3J,M) (Krauss et al., 1993; Schulte-Merker et al., 1994). In 2-somite-stage complete shield-ablated embryos, staining with *hlx-1* revealed a complete loss of prechordal plate (Fig. 5J) (Fjose et al., 1994). Consistent with a role for the notochord in somite patterning, the somites, though segmented, formed compressed rectangles instead of characteristic chevrons (Fig. 3I). The chevron shape of somites is controlled by muscle pioneer cells, a special group of *engrailed*-expressing muscle cells that form at the horizontal myoseptum. Except for regions where a few notochord cells remained, *engrailed-1* (*en1*) expression was abolished in complete shield-ablated embryos (Fig. 3L) (Ekker et al., 1992). By contrast, *en1* expression at the midbrain-hindbrain boundary was normal (data not shown). Hence, we conclude that complete removal of the shield region early in development leads to a complete loss of shield-derived tissues at later stages. In addition, notochord dependent patterning fails to occur. Despite complete removal of shield tissue, the embryonic axis forms and has clear AP patterning.

CNS defects

Given the known roles for axial mesendoderm in patterning the neurectoderm, we examined the dorsal-ventral organization of the CNS in complete shield-ablated embryos (van Straaten et al., 1988; Yamada et al., 1991). We found that 56% of these

embryos were cyclopean ($n=70$) (Fig. 4F). This defect correlates with a loss of ventral neurectoderm throughout the body axis, as seen by the reduction in *tiggy winkle hedgehog* (*twh*) and *shh* expression, both of which mark medial floor plate cells and the ventral brain (Fig. 4G,H) (Ekker et al., 1995). We also investigated the effect of axial tissue loss on motorneuron specification in complete shield-ablated embryos. The antibody Znp1 marks primary neurons and their ventral root axonal projections (Trevarrow et al., 1990). Complete shield-ablated embryos lacked motorneuron ventral root projections (Fig. 4I). At the neural plate stage, *islet-1* (*isl-1*) marks all primary neurons of the forming spinal cord (Inoue et al., 1994). Laterally, *isl-1* marks Rohon-Beard sensory neurons and medially, it marks motorneurons. We found Rohon-Beard sensory neurons to be present in complete shield-ablated embryos while motorneurons were either absent or severely reduced in number, forming at most a single sparse column at the midline (Fig. 4J). Hence as with *boz* mutants, ventral patterning of the CNS is disrupted in complete shield-ablated embryos (Fekany et al., 1999).

AP patterning in *boz* mutant embryos is disrupted in at least two ways. First, severely affected *boz* mutant embryos fail to form the most anterior CNS tissues, as revealed by the loss of *emx1* expression (Fekany et al., 1999; Houart et al., 1998; Morita et al., 1995). Second, rhombomeres 3 and 5 are expanded along the AP axis, as shown by *EphA4* expression (Fekany et al., 1999; Xu et al., 1994). We therefore examined the AP patterning of complete shield-ablated embryos using *EphA4*, *emx1* and *zanf*, a marker of the zebrafish telencephalon homologous to the mouse *Hesx1* gene (Kazanskaya et al., 1997; Thomas and Beddington, 1996). In complete shield-ablated embryos *EphA4* expression at 24 hpf revealed an AP expansion of rhombomeres 1, 3 and 5 (Fig. 5F). Although head morphology was clearly abnormal, we found *emx1* still to be expressed in complete shield-ablated embryos at 24 hpf (Fig. 5H). At the 2-somite-stage of development, the *emx1* expression domain was compressed toward the midline of complete shield-ablated embryos, but occupying an area of

Fig. 4. Ventral patterning of the CNS is disrupted in complete shield-ablated embryos. (A-E) Control embryos. (F) Complete shield-ablated embryos become cyclopean. (G,H) The reduction of ventral neurectoderm in complete shield-ablated embryos is reflected by the reduction in *twh* and *shh* expression, which mark the midline floor plate cells and the ventral brain. The arrow shows remaining floor plate cells. (I) *znp1* reveals the absence of motorneuron ventral root projections (shown by arrow in D) in complete shield-ablated embryos. (J) In complete shield-ablated embryos, *isl-1* expression is severely reduced in medial motorneurons (shown by arrow in E) and normal in the lateral Rohon-Beard sensory neurons. (A,C,D,F,H,I) Lateral views of 24 hpf embryos with anterior to the left. (B,G) Lateral views of 18 hpf embryos with anterior to the left. (E,J) Dorsal views of 5-somite-stage embryos with anterior up.

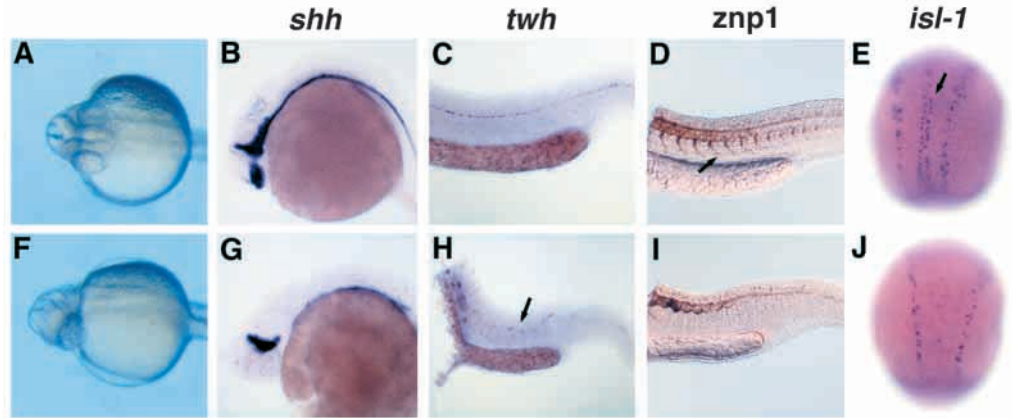
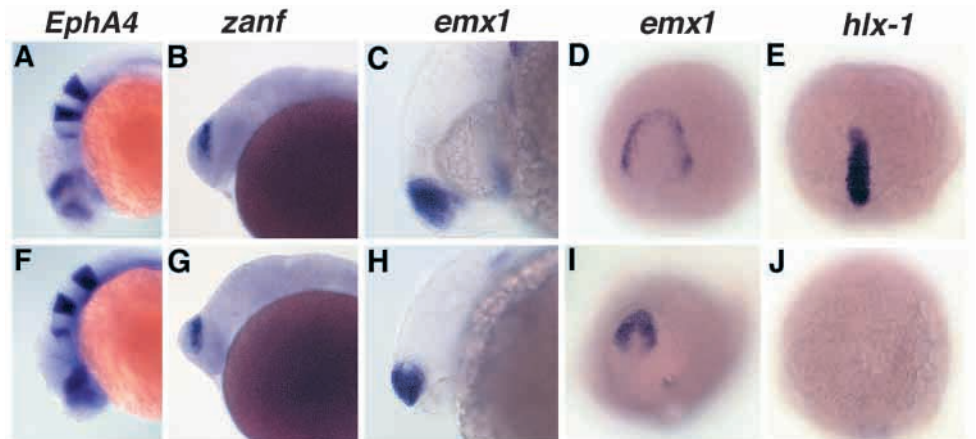


Fig. 5. In complete shield-ablated embryos AP patterning is not severely affected. (A-E) Control embryos. (F) After complete shield removal, *EphA4* expression in rhombomeres 1, 3 and 5 is slightly expanded. (G-I) In complete shield-ablated embryos, the telencephalon is patterned, as revealed by *zanf* and *emx1* expression. (J) *hlx-1* expression is absent in complete shield-ablated embryos, confirming the loss of prechordal plate tissue in the head. (A-C,F-H) Lateral views of 24 hpf embryos with anterior to the left. (D,E,I,J) Dorsal views of 2-somite-stage embryos with anterior up.



similar size to that of controls (Fig. 5I). Finally, we found that *zanf* is expressed in complete shield-ablated embryos, further indicating that the telencephalon is specified (Fig. 5G). Similar to the AP patterning defects seen in *boz* mutant embryos we find the rhombomeres to be expanded. In contrast, however, we find that shield ablation does not prevent the formation of the most anterior neurectodermal tissues. Taken together these results suggest that, by the time we remove organizer tissue, the organizer has already acted both to specify and to impart AP pattern to the neurectoderm.

Factors affecting regeneration of shield derivatives following shield removal

As described above, we found that a large percentage of embryos developed normally after removal of the morphological shield. To understand events underlying regeneration of shield derivatives, we investigated the role of wound healing immediately following shield removal. We challenged the efficacy of wound closure by performing shield removals in solutions of several different salt concentrations. The removal of the morphologically defined shield in 1× Danieau solution, which has a salt concentration similar to interstitial fluid, allowed the recovery of a high percentage of embryos (71%), as is reported above. By contrast, shield

removal in 0.3× or 0.1× Danieau solution yields a much reduced percentage of normal embryos: 37% (18/48 embryos) and 44% (16/36 embryos), respectively. When the organizer was completely removed there was only a small difference in the percentage of normal embryos: 6% (4/70 embryos), 6% (2/34 embryos) and 8% (1/13 embryos), obtained after operating in 1×, 0.3× and 0.1× Danieau solution, respectively. One possible explanation is that shield regeneration is not only dependent upon the presence of residual lateral shield cells but also upon their proper re-association across the extirpated domain after shield removal. To test the possibility that solutions of differing osmotic strengths modify cellular reassociation dynamics after shield removal, we examined embryos by scanning electron microscopy after shield removal in 0.3× Danieau or 1× Danieau solution. We found that in 0.3× Danieau solution the wound was covered with cells within 10 minutes, while those operated on in 1× Danieau solution took more than twice as long to heal (Fig. 6).

The shield is able to induce the formation of a complete secondary axis

Complete shield removal experiments suggest that the organizer acts to induce and pattern the embryonic axis prior to shield stage. Further, we know that if only the morphological

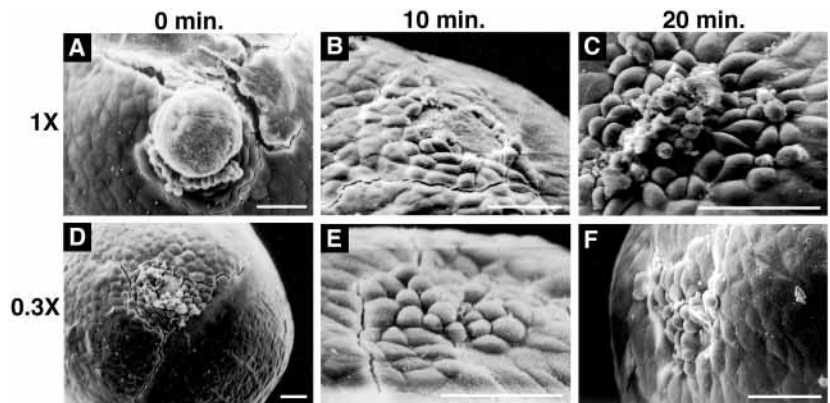


Fig. 6. Scanning electron micrographs of 6 hpf embryos after shield removal. (A,D) A wound immediately after shield removal performed in 1× and 0.3× Danieau solution. (B,E) Shown are the wounds of shield-ablated embryos 10 minutes post-surgery in 1× or 0.3× Danieau solution. Healing seems to occur more rapidly in 0.3× Danieau solution. (C,F) The wounds of shield-ablated embryos are healed after 20 minutes in either 1× or 0.3× Danieau solution. Bars, 50 μm.

shield is removed, embryos will recover. It has been reported that shields dissected at the stage we have investigated (6 hpf) can only induce partial second axes when transplanted to ventral or lateral regions of a host embryo (Shih and Fraser, 1996). These partial axes possessed all tissues posterior to the otic vesicle, and occasionally included secondary hearts, but never eyes or telencephalon (Shih and Fraser, 1996). We therefore sought to determine whether 6 hpf morphological shields obtained by our methodology induce complete or partial second axes.

Morphologically defined shields were removed from dextran-labeled 6 hpf embryos and transplanted into the ventral germ-ring of 6 hpf host embryos. Experimental embryos were cultured until 24 hpf and analyzed. The inductive potential of the grafted shield was compared with that of ventral germ-ring grafts of similar size. We found that shield grafts could induce a complete secondary axis, with eyes and a beating heart in $51 \pm 9\%$ of shield-to-ventral margin grafts ($n=151$) (Fig. 7; Table 1). Invariably, the anterior end of the secondary axis was oriented facing the animal pole. The anteriormost part of the secondary axis, however, could be at a distance from the anteriormost part of the primary axis (Fig. 7A,B) or immediately adjacent (Fig. 8A). In addition, secondary axes were found at all angles from the primary axis ranging from 180° (Fig. 8A) to immediately adjacent or overlapping (data not shown).

The anterior patterning of induced complete secondary axes was examined using *EphA4* (Fig. 7D,E) and *emx1* (Fig. 7F,G). *EphA4* expression was detected in all complete secondary axes analyzed ($n=18$), indicating the proper induction and patterning of both diencephalon and rhombencephalon (Fig. 7D,E). In addition, *emx1* was expressed in all complete secondary axes ($n=8$), indicating that the telencephalon is present in the induced axes (Fig. 7F,G). We also find that the presence of a fully patterned forebrain and hindbrain is independent of the position of the secondary axis (compare Fig. 7D,F with E,G).

The fate of transplanted tissue was followed in living embryos using fluorescent-dextran lineage tracer dye. We found donor shield tissue contributed predominantly to the hatching gland, prechordal plate, hypochord, notochord and floor plate of secondary axes (Figs 7A,B, 8A,B). These tissues appeared to be entirely donor derived. In addition, a few donor-derived cells were found scattered throughout the ventral nervous system and throughout the overlying ectoderm of the secondary axes (Fig. 8D). The vast majority of tissues in the

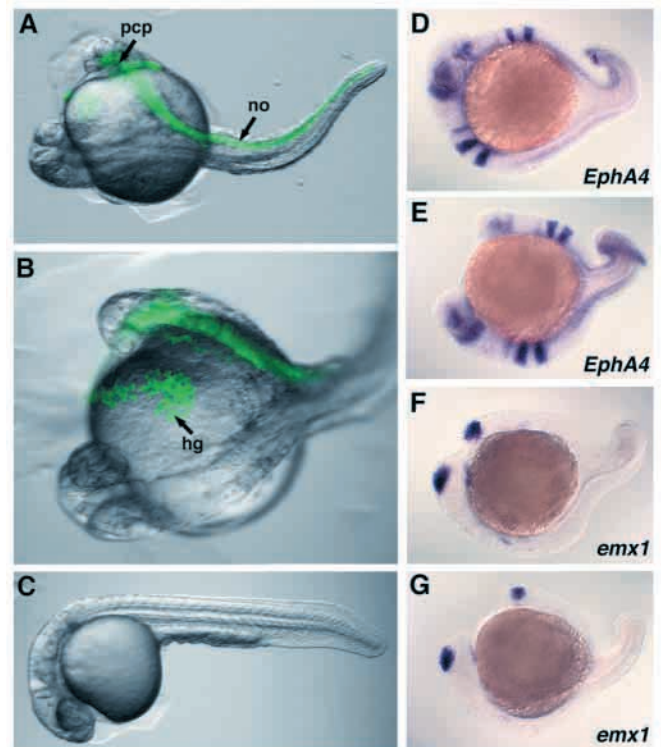


Fig. 7. Transplantation of the embryonic shield to the ventral side of a host embryo. (A,B) A morphologically defined shield, derived from a 6 hpf embryo, is able to induce a complete secondary axis when transplanted to the ventral side, within the germ-ring. The induced secondary axes possess the most anterior structures including a normal head with two eyes. (C) A Nomarski image showing that the shield donor embryo developed completely normal. (D,E) In a complete secondary axis, the diencephalon is normally patterned, as revealed by *EphA4* expression in the presumptive dorsal thalamus and the region adjacent to the otic vesicles. The rhombencephalon is also normally patterned, as revealed by the expression of *EphA4* in rhombomeres 1, 3 and 5. (F,G) The telencephalon of a complete secondary axis is normally patterned, as revealed by *emx1* expression. (D-G) Lateral views of 24 hpf embryos with anterior to the left and induced secondary axis up. no, notochord; pcp, prechordal plate; hg, hatching gland.

secondary axis, including the brain, dorsal spinal cord and somites, however, were not labeled and therefore derived from host blastoderm. Hence, even though the organizer has already

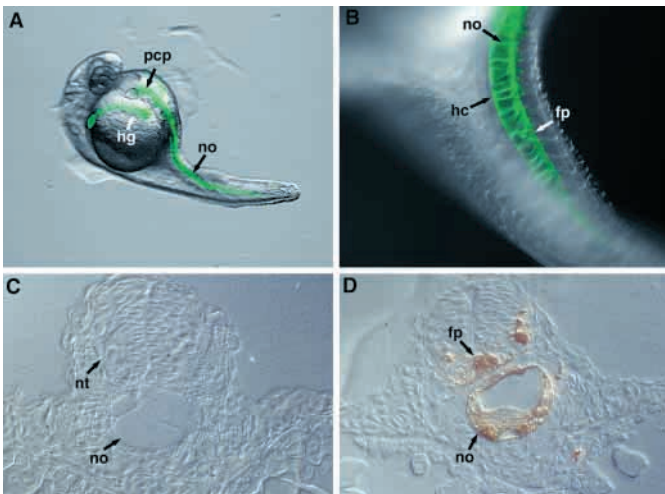


Fig. 8. Fate of transplanted shield tissue. (A) Using epifluorescence it is possible to determine the contribution of the shield tissue to notochord, prechordal plate and hatching gland. (B) A higher magnification of the tail shows labeled cells in the notochord, hypochord and floor plate. (C) A histological section through the primary axis showing the notochord and the neural tube completely devoid of labeled tissue. (D) A histological section through the secondary axis shows that the labeled shield cells (green) become notochord and floor plate. The majority of the neuroectoderm, however, is free of labeled cells. no, notochord; pcp, prechordal plate; hg, hatching gland; fp, floor plate; hc, hypochord; nt, neural tube.

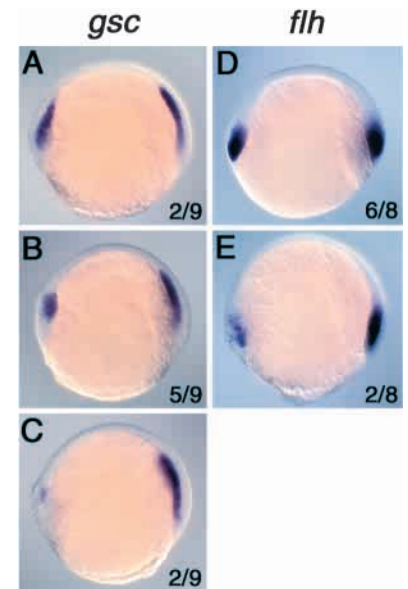
acted by the time of shield removal, the shield tissue retains the capacity to induce a complete secondary axis. Moreover, the fates of shield-derived cells in these secondary axes are identical to the fates of normal shield-derived cells, determined either by homotopic transplantation or by cell labeling (data not shown) (Shih and Fraser, 1995, 1996).

Embryonic shield fragments enriched for deep *gsc*-expressing cells can induce secondary axes possessing only anterior structures

The notion of separable head and trunk organizer activities derives from the initial experiments of Spemann (Spemann and Mangold, 1924). A recent study has shown that the *Xenopus* organizer is partitioned along its AP axis into two functionally and developmentally distinct regions. The anterior organizer is able to induce a secondary axis possessing only anterior

Fig. 9. Expression of *gsc* and *flh* in embryos that received a shield graft. (A-C) *gsc*-expression in the primary and secondary induced axis. (A) The amount of *gsc*-expressing tissue in the transplant is roughly equal to that of the endogenous shield in 22% ($n=9$) of the cases. (B) In 56% of the cases ($n=9$) the amount of *gsc*-expressing tissue in the transplant correspond to approximately half of the endogenous shield. (C) A few or no *gsc*-expressing cells were found in the

transplanted tissue in 22% of the cases ($n=9$). (D,E) *flh* expression in the endogenous and transplanted shields. (D) The amount of *flh*-expressing tissue in the transplanted shield is equal to the endogenous shield in 75% ($n=8$) of cases. (E) In 25% ($n=8$) the amount of *flh*-expressing tissue in the transplant is approximately half of the endogenous shield. All panels show endogenous shield to the right and transplanted shield to the left.



structures, while the posterior organizer can induce secondary axes uniquely possessing posterior structures (Zoltewicz and Gerhart, 1997). In the transplantation experiments presented here, 51% of the shield grafts were able to induce a complete secondary axis. The remaining secondary axes were incomplete, ranging from some that possessed a head lacking eyes (21%) to some possessing only a trunk and tail (2%) (see Table 1). In situ hybridization studies performed 20 minutes after shield transplantation revealed that cells expressing *flh* were efficiently transplanted in every case ($n=8$), whereas cells expressing *gsc* were transplanted 78% of the time ($n=9$) (Fig. 9). These results suggest that the zebrafish organizer is also regionalized. Further, the results suggest that a combination of deep *gsc*-expressing cells and superficial *flh*-expressing cells is required to obtain complete secondary axes.

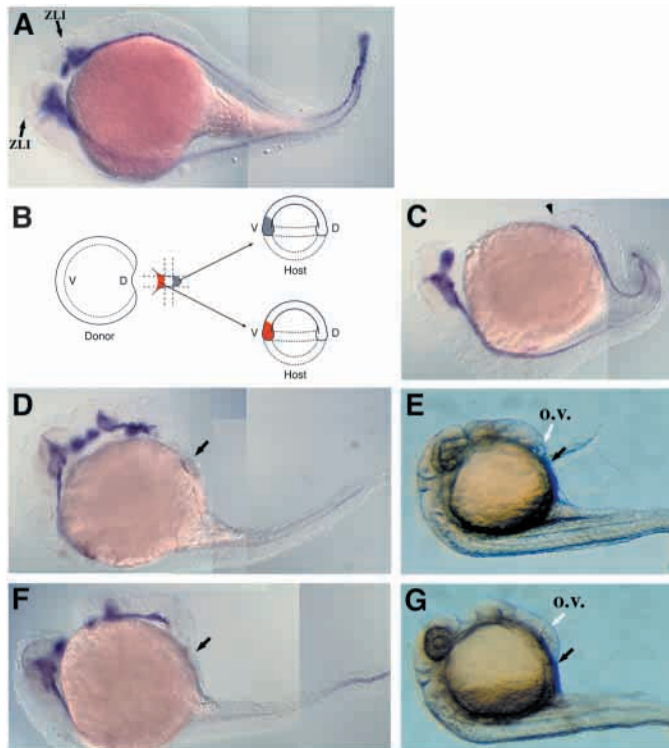
To test directly whether deep and superficial regions of the

Table 1. Transplantation of the embryonic shield to the ventral side of a 6 hpf embryo

	Number induced											% 51±9
	15	1	4	13	8	18	4	5	2	3	5	
Secondary axis complete	15	1	4	13	8	18	4	5	2	3	5	
Secondary axis incomplete												
Telenceph.	3	0	0	0	0	0	7	4	3	5	5	21±8
Inc. heart	8	6	0	6	1	2	0	0	0	0	0	14±7
Inc. o.v.	0	1	0	1	0	0	0	1	0	0	3	4±2
Trunk only	2	0	0	1	0	0	0	0	0	0	1	2±1
No induction	4	0	0	0	0	0	0	4	4	0	1	8±4
Total grafts	32	8	4	21	9	20	11	14	9	8	15	

%, average of the percentage of each experiment ± s.e.m.

Telenceph., an embryo with telencephalon, as defined by the presence of *emx1*, but no eyes; inc. heart, an embryo with no forebrain, but with a beating heart; inc. o.v., an embryo induced anterior only to the level of the otic vesicle.



shield have distinct organizer properties, we separated deep and superficial shield tissue and then transplanted these fragments into the ventral side of host embryos (Fig. 10B). Both superficial (schematic, gray piece in Fig. 10B) and deep (schematic, red piece in Fig. 10B) fragments induced secondary axes. We observed, however, a qualitative difference between secondary axes induced by deep versus superficial shield fragments. Secondary axes possessing only a head (Fig. 10D-G) were often obtained when deep fragments were grafted (Table 2). By contrast, a high proportion of secondary axes induced by superficial shield fragments comprised only posterior structures (Fig. 10C and Table 2). These data suggest that anterior and posterior organizer activities of the zebrafish

Fig. 10. Transplantation of deep versus superficial fragments of the embryonic shield. (A) The morphologically defined shield is able to induce a complete secondary axis. The expression of *shh* can be detected in the ventral midline of the brain, in the zona limitans intrathalamica (ZLI) and in the floor plate of the trunk and tail. (B) Schematic diagram of the dissection of the shield to obtain separate deep and superficial shield fragments for transplantation. The dotted lines represent cuts made with an eyebrow-hair knife into an aspirated shield. The gray area corresponds to the superficial cells and the red area to the deep cells. (C) An example of a secondary axis lacking head structures (arrowhead) induced by one superficial shield fragment. In these anterior-truncated secondary axes the expression of *shh* is restricted to the floor plate of the trunk and tail. No *shh* expression characteristic of the head is seen. (D-G) An example of a secondary axis lacking trunk and tail induced by two deep shield fragments. (D,F) The presence of a normally patterned head is revealed by the expression of *shh* in the ventral brain and the ZLI. The absence of trunk (arrow) is revealed by the interruption of *shh* expression in the floor plate at the level of the otic vesicle (o.v.). (E,G) Live Nomarski images of the embryos stained in D and F showing that the induced heads are complete with eyes and otic vesicles.

embryonic shield are separable. We correlated these distinct inducing activities with differential expression of *gsc* and *flh*. In situ hybridization studies performed 20 minutes after deep and superficial shield fragment transplantation showed that nearly all deep shield fragment transplants contain a high proportion of *gsc*-expressing cells and in some cases have few or no *flh*-expressing cells. Similarly, most superficial fragment transplants have a high proportion of *flh*-expressing cells and in some cases have few or no *gsc*-expressing cells (Table 3).


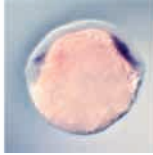
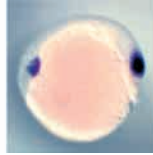
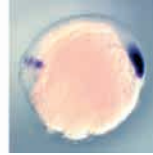
The persistence of *gsc*-expressing cells in superficial grafts (and *flh* expressing cells in deep grafts) probably reflects technical limits in our ability to separate these two shield regions. The partial impurity of our deep and superficial fragments might explain the fact that both types of fragment can sometimes induce complete secondary axes (Table 2). We were able to overcome the contamination of superficial grafts with *gsc*-expressing cells by transplanting cells from the region adjacent to the morphological shield. Nearly all transplants of lateral fragments contained only *flh*-expressing cells (Table 3)

Table 2. Transplantation of deep, superficial and lateral shield fragments to the ventral side of a 6 hpf embryo

		Anterior only	Posterior only	Anterior and posterior
1 piece	Deep	11/21	6/21	4/21
	Superficial	1/26	14/26	11/26
	Lateral	0/67	64/67	3/67
2 pieces	Deep	6/16	2/16	8/16
	Superficial	0/9	7/9	2/9
	Lateral	0/16	13/16	3/16

o.v., otic vesicle; anterior only, telencephalon through o.v.; posterior only, heart (or o.v.) through tail; anterior and posterior, complete axis. The telencephalon did not always include eyes. The tail begins posterior to the yolk extension.

Table 3. Expression of *gsc* and *flh* in embryos that have received shield fragment grafts

					
Fragment		High <i>gsc</i>	Low or absent <i>gsc</i>	High <i>flh</i>	Low or absent <i>flh</i>
1 piece	Deep	5/5	0/5	3/5	2/5
	Superficial	4/8	4/8	6/10	4/10
	Lateral	0/11	11/11*	6/15	9/15
2 pieces	Deep	3/5	2/5	4/5	1/5
	Superficial	2/4	2/4	4/6	2/6
	Lateral	1/9	8/9	5/8	3/8

Pictures are oriented with endogenous shield to the right and transplanted fragments to the left.
**gsc* expression was absent in all embryos.

and the vast majority of axes they induced consisted of posterior structures only (Table 2).

The dissected fragments represent only a fraction of the endogenous *gsc*- or *flh*-expressing cells in the shield region. To ensure that the observed differences in induced axes were not a simple consequence of limited quantity transplant tissue, we performed additional transplants. We find that a two piece graft of each fragment type has the same axis-inducing activity and the same profile of *gsc* and *flh* expression as the corresponding single piece graft (Tables 2, 3). We did, however, find that axes induced by one piece were generally smaller than axes induced by two pieces (data not shown). We conclude that is not the quantity but rather the quality of fragments that determines whether anterior or posterior structures are induced.

DISCUSSION

Complete shield ablation phenocopies the *bozok* mutation

When the shield region is completely removed the normal derivatives of the shield fail to form. The dorsal organizer, however, has already acted to induce neuroectoderm and to impart anterior-posterior (AP) pattern. The set of defects resulting from complete removal of shield is virtually identical to the phenotype of severely affected *boz* mutants. We conclude therefore that the *boz* gene product primarily specifies axial mesendoderm and is not involved in the specification of organizer activity per se. In shield-removal experiments we are able to separate two distinct organizer activities, namely induction of embryonic axes and formation of axial mesendoderm. Similarly, the *boz* mutation highlights the separable nature of these activities at the earliest stages of organizer specification. The *boz* gene product is expressed in the yolk-syncytial layer, apparently in response to the earliest dorsal signals mediated by β -catenin. The *boz* gene product or a similar activity is required for proper specification of the axial mesendoderm, but is not directly required for neural induction. The most severely affected *boz* mutants, representing a small percentage, display AP patterning defects in the central nervous system (CNS), seen as a broadening of rhombomeres and loss of telencephalon and ventral diencephalon in the forebrain (Fekany et al., 1999). We expect that this infrequent

loss of anterior neuroectoderm results from the failure to specify prechordal mesendoderm prior to shield stage, as seen from the downregulation of *gsc* in *boz* mutant embryos (Fekany et al., 1999). We expect the reason shield-ablated embryos are able to specify anterior neuroectoderm while some *boz* mutants are not is an issue of timing. Specifically, since we rely on shield morphology to guide the removal of tissue we are unable to ablate the shield until nearly 1 hour after organizer-specific genes are first expressed. We would therefore predict that removal of organizer prior to morphological shield formation would lead to anterior defects similar to those seen in severe *boz* mutant embryos. Indeed removal of dorsal marginal tissue at 40% epiboly was found to result in the loss of *odd-paired like* (*opl*) expression during the neural plate stage (Grinblat et al., 1998).

Morphological shield removal does not significantly affect development

We found that shield derivatives were able to regenerate only after morphological shield removal in which some lateral *gsc*- and *flh*-expressing cells were left. Such regeneration after morphological shield removal is dependent upon appropriate wound healing, which is itself dependent on the ionic balance of the experimental medium. Initially, we performed the shield removal experiments in 0.3 \times Danieau solution and found that the majority of embryos did not properly generate axial mesendoderm. We propose that the EVL cells, which are rapidly moving to seal the embryo from the low-salt extra-embryonic condition, form a scar that prevents the coalescence of deep cells. In the high-salt condition, according to this model, EVL cells fail to rapidly close the wound and deep cells are able to reassociate and go on to regenerate normal shield derivatives.

There have been several reports of extensive renewal of Hensen's node and its derivatives after surgical removal of Hensen's node and the rostral part of the primitive streak (Psychoyos and Stern, 1996; Yuan and Schoenwolf, 1999; Joubin and Stern, 1999). A recent study of the chicken organizer describes the continuous renewal of organizer tissue as development proceeds (Joubin and Stern, 1999). Specifically, a region of the embryo is described that induces organizer fate to otherwise unspecified tissue as it passes through the node. In contrast to the situation in avian embryos,

there is no evidence that regeneration of organizer derivatives occurs in *Xenopus* or mouse embryos (Cooke, 1985; Davidson et al., 1999). The fact that we observe regeneration after shield removal only if tissue lateral to the morphological shield is left behind, taken together with the observations in mouse and *Xenopus*, suggest that continuous organizer renewal is unique to the avian embryo.

Induction of complete second axes by morphological shield transplantation

By contrast to a recent study, we find that a transplanted shield is capable of inducing a complete second axis (Shih and Fraser, 1996). This discrepancy may be due to differences in the transplantation methods employed. In order to obtain proper induction of the head we believe it is important to transplant the deeper *gsc*-expressing cells of the shield. For zebrafish, the use of an eyebrow hair knife to remove shield tissue may prevent the removal of the deep cells. These cells reside immediately adjacent to the yolk cell and aggressive manipulations will result in the puncture of the yolk cell and collapse of the embryo. The method we describe here allows complete removal of the deep cells by suction, leaving the yolk cell intact. Using this method we were able to test directly the inductive properties of deep versus superficial shield tissue. When the shield is divided into fragments and the deep cells are transplanted into the ventral side of a host embryo it is possible to obtain second axes with complete heads that lack posterior structures. With superficial fragment transplants it is possible to obtain second axes possessing posterior structures but lacking heads. These results are consistent with an earlier study of the organizer activities of teleost embryonic shield, in which transplantation of anterior fragments of the mid-gastrula *Fundulus* shield induced the formation of head structures in the absence of trunk mesoderm (Oppenheimer, 1953). Taken together these results suggest that the quality of signaling imparted by the deep shield tissue is required for normal head formation. The mechanical approach we used to obtain deep versus superficial shield grafts, however, does not allow consistent separation of *gsc*-expressing and *flh*-expressing tissue. We found that deep grafts were often contaminated with *flh*-expressing cells. Similarly, superficial grafts were often contaminated with *gsc*-expressing cells. In the future, through the use of transgenic embryos expressing green fluorescent protein (GFP) under the control of *gsc* or *flh* promoters, a more precise separation of the deep and superficial shield fragments should be practicable.

It has been suggested that it is not the quality of organizer tissue that governs whether head will form but the position of the transplant (Koshida et al., 1998). These investigators found that the animal cap tissue is imbued with a propensity to express anterior neural fate. They also found that transplantation of shield, Hensen's node, or Noggin/Chordin expressing COS7 cells could induce neurectoderm formation if transplantation was near the animal pole rather than at the margin. In contrast to these results, we find that transplantation of shield to the margin is sufficient to obtain complete second axes. Furthermore, when the entire organizer is removed at late blastula to early gastrula stages no *opl* expression was observed, indicating that this region is crucial for initial forebrain patterning (Grinblat et al., 1998). Therefore, while the animal cap shows a propensity to take on anterior neural

fates it is clearly not committed to such fates, nor can these fates be manifest without a dorsal/marginal signal such as that emanating from the shield.

The authors wish to thank Benjamin Feldman, Jean-Paul Vincent, Rosa Beddington and Jim Smith for a critical reading of the manuscript. L. Saúde was supported by a PhD studentship from Fundação para a Ciência e a Tecnologia, Programa PRAXIS XXI.

REFERENCES

- Beddington, R. S.** (1994). Induction of a second neural axis by the mouse node. *Development* **120**, 613-20.
- Cooke, J.** (1985). Dynamics of the control of body pattern in the development of *Xenopus laevis*. III. Timing and pattern after u.v. irradiation of the egg and after excision of presumptive head endo-mesoderm. *J. Embryol. Exp. Morph.* **88**, 135-50.
- Davidson, B. P., Kinder, S. J., Steiner, K., Schoenwolf, G. C. and Tam, P. P.** (1999). Impact of node ablation on the morphogenesis of the body axis and the lateral asymmetry of the mouse embryo during early organogenesis. *Dev. Biol.* **211**, 11-26.
- Doniach, T., Phillips, C. R. and Gerhart, J. C.** (1992). Planar induction of anteroposterior pattern in the developing central nervous system of *Xenopus laevis*. *Science* **257**, 542-5.
- Ekker, M., Wegner, J., Akimenko, M. A. and Westerfield, M.** (1992). Coordinate embryonic expression of three zebrafish engrailed genes. *Development* **116**, 1001-10.
- Ekker, S. C., Ungar, A. R., Greenstein, P., von Kessler, D. P., Porter, J. A., Moon, R. T. and Beachy, P. A.** (1995). Patterning activities of vertebrate hedgehog proteins in the developing eye and brain. *Curr. Biol.* **5**, 944-55.
- Fekany, K., Yamanaka, Y., Leung, T., Sirotkin, H. I., Topczewski, J., Gates, M. A., Hibi, M., Renucci, A., Stemple, D., Radbill, A., Schier, A. F., Driever, W., Hirano, T., Talbot, W. S. and Solnica-Krezel, L.** (1999). The zebrafish *bozozok* locus encodes Dharma, a homeodomain protein essential for induction of gastrula organizer and dorsoanterior embryonic structures. *Development* **126**, 1427-1438.
- Fjose, A., Izpissua-Belmonte, J. C., Fromental-Ramain, C. and Duboule, D.** (1994). Expression of the zebrafish gene *hlx-1* in the prechordal plate and during CNS development. *Development* **120**, 71-81.
- Grinblat, Y., Gamse, J., Patel, M. and Sive, H.** (1998). Determination of the zebrafish forebrain: induction and patterning. *Development* **125**, 4403-16.
- Gritsman, K., Talbot, W. S. and Schier, A. F.** (2000). Nodal signaling patterns the organizer. *Development* **127**, 921-32.
- Harland, R. and Gerhart, J.** (1997). Formation and function of Spemann's organizer. *Annu. Rev. Cell Dev. Biol.* **13**, 611-667.
- Houart, C., Westerfield, M. and Wilson, S. W.** (1998). A small population of anterior cells patterns the forebrain during zebrafish gastrulation. *Nature* **391**, 788-92.
- Inoue, A., Takahashi, M., Hatta, K., Hotta, Y. and Okamoto, H.** (1994). Developmental regulation of islet-1 mRNA expression during neuronal differentiation in embryonic zebrafish. *Dev. Dyn.* **199**, 1-11.
- Joubin, K. and Stern, C. D.** (1999). Molecular interactions continuously define the organizer during the cell movements of gastrulation. *Cell* **98**, 559-571.
- Karnovsky, M. J.** (1965). A formaldehyde-glutaraldehyde fixative of high osmolality for use in electron microscopy. *J. Cell Biol.* **27**, 137-138.
- Kazanskaya, O. V., Severtzova, E. A., Barth, K. A., Ermakova, G. V., Lukyanov, S. A., Benyumov, A. O., Pannese, M., Boncinelli, E., Wilson, S. W. and Zaraisky, A. G.** (1997). Anf: a novel class of vertebrate homeobox genes expressed at the anterior end of the main embryonic axis. *Gene* **200**, 25-34.
- Keller, R., Shih, J., Sater, A. K. and Moreno, C.** (1992). Planar induction of convergence and extension of the neural plate by the organizer of *Xenopus*. *Dev. Dyn.* **193**, 218-34.
- Kimmel, C. B., Ballard, W. M., Kimmel, S. R., Ullmann, B. and Schilling, T. F.** (1995). Stages of embryonic development of the zebrafish. *Dev. Dyn.* **203**, 253-310.
- Koshida, S., Shinya, M., Mizuno, T., Kuroiwa, A. and Takeda, H.** (1998). Initial anteroposterior pattern of the zebrafish central nervous system is determined by differential competence of the epiblast. *Development* **125**, 1957-66.

- Krauss, S., Concordet, J. P. and Ingham, P. W.** (1993). A functionally conserved homolog of the *Drosophila* segment polarity gene *hh* is expressed in tissues with polarizing activity in zebrafish embryos. *Cell* **75**, 1431-44.
- Morita, T., Nitta, H., Kiyama, Y., Mori, H. and Mishina, M.** (1995). Differential expression of two zebrafish *emx* homeoprotein mRNAs in the developing brain. *Neurosci. Lett.* **198**, 131-4.
- Oppenheimer, J. M.** (1936). Transplantation experiments on developing teleosts (*Fundulus* and *Perca*). *J. Exp. Zool.* **72**, 409-437.
- Oppenheimer, J. M.** (1953). The development of transplanted fragments of *Fundulus* gastrulae. *Proc. Natl. Acad. Sci. USA* **39**, 1149-1152.
- Psychoyos, D. and Stern, C. D.** (1996). Restoration of the organizer after radical ablation of Hensen's node and the anterior primitive streak in the chick embryo. *Development* **122**, 3263-73.
- Rowning, B. A., Wells, J., Wu, M., Gerhart, J. C., Moon, R. T. and Larabell, C. A.** (1997). Microtubule-mediated transport of organelles and localization of beta-catenin to the future dorsal side of *Xenopus* eggs. *Proc. Natl. Acad. Sci. USA* **94**, 1224-9.
- Schulte-Merker, S., van Eeden, F. J., Halpern, M. E., Kimmel, C. B. and Nusslein-Volhard, C.** (1994). *no tail* (*ntl*) is the zebrafish homologue of the mouse *T* (*Brachyury*) gene. *Development* **120**, 1009-15.
- Shih, J. and Fraser, S. E.** (1995). Distribution of tissue progenitors within the shield region of the zebrafish gastrula. *Development* **121**, 2755-65.
- Shih, J. and Fraser, S. E.** (1996). Characterizing the zebrafish organizer: microsurgical analysis at the early-shield stage. *Development* **122**, 1313-22.
- Smith, J. C. and Slack, J. M.** (1983). Dorsalization and neural induction: properties of the organizer in *Xenopus laevis*. *J. Embryol. Exp. Morph.* **78**, 299-317.
- Spemann, H. and Mangold, H.** (1924). Über die Induktion von Embryonalanlagen durch Implantation artfremder Organisatoren. *Wilhelm Roux Arch. Entw. Mech. Org.* **100**, 599-638.
- Stachel, S. E., Grunwald, D. J. and Myers, P. Z.** (1993). Lithium perturbation and goosecoid expression identify a dorsal specification pathway in the pregastrula zebrafish. *Development* **117**, 1261-74.
- Talbot, W. S., Trevarrow, B., Halpern, M. E., Melby, A. E., Farr, G., Postlethwait, J. H., Jowett, T., Kimmel, C. B. and Kimelman, D.** (1995). A homeobox gene essential for zebrafish notochord development. *Nature* **378**, 150-7.
- Tam, P. P. and Steiner, K. A.** (1999). Anterior patterning by synergistic activity of the early gastrula organizer and the anterior germ layer tissues of the mouse embryo. *Development* **126**, 5171-9.
- Thisse, C. and Thisse, B.** (1998). High resolution whole-mount in situ hybridization. *Zebrafish Sci. Mon.* **5**, 8-9.
- Thomas, P. and Beddington, R.** (1996). Anterior primitive endoderm may be responsible for patterning the anterior neural plate in the mouse embryo. *Curr. Biol.* **6**, 1487-96.
- Trevarrow, B., Marks, D. L. and Kimmel, C. B.** (1990). Organization of hindbrain segments in the zebrafish embryo. *Neuron* **4**, 669-79.
- van Straaten, H. W., Hekking, J. W., Wiertz-Hoessels, E. J., Thors, F. and Drukker, J.** (1988). Effect of the notochord on the differentiation of a floor plate area in the neural tube of the chick embryo. *Anat. Embryol.* **177**, 317-24.
- Varlet, I., Collignon, J. and Robertson, E. J.** (1997). *nodal* expression in the primitive endoderm is required for specification of the anterior axis during mouse gastrulation. *Development* **124**, 1033-44.
- Vincent, J. P., Oster, G. F. and Gerhart, J. C.** (1986). Kinematics of gray crescent formation in *Xenopus* eggs: the displacement of subcortical cytoplasm relative to the egg surface. *Dev. Biol.* **113**, 484-500.
- Waddington, C. H.** (1932). Experiments on the development of the chick and the duck embryo cultivated in vitro. *Proc. Trans. R. Soc. Lond. B* **211**, 179-230.
- Xu, Q., Holder, N., Patient, R. and Wilson, S. W.** (1994). Spatially regulated expression of three receptor tyrosine kinase genes during gastrulation in the zebrafish. *Development* **120**, 287-99.
- Yamada, T., Placzek, M., Tanaka, H., Dodd, J. and Jessell, T. M.** (1991). Control of cell pattern in the developing nervous system: polarizing activity of the floor plate and notochord. *Cell* **64**, 635-47.
- Yuan, S. and Schoenwolf, G. C.** (1999). Reconstitution of the organizer is both sufficient and required to re-establish a fully patterned body plan in avian embryos. *Development* **126**, 2461-73.
- Zoltewicz, J. S. and Gerhart, J. C.** (1997). The Spemann organizer of *Xenopus* is patterned along its anteroposterior axis at the earliest gastrula stage. *Dev. Biol.* **192**, 482-91.